Numerical Investigation of a Dual-Tank Drain System under Marine Environment

Hyeon Ji Kim, In Cheol Bang*
Department of Nuclear Engineering, Ulsan National Institute of Science and Technology (UNIST), 50 UNIST-gil, Ulju-gun, Ulsan, 44949, Republic of Korea
**Corresponding author: icbang@unist.ac.kr*

Keywords : Molten Salt Reactor, Drain System, Rolling motion, Computational Fluid Dynamics.

1. Introduction

Driven by urgent decarbonization goals, the maritime sector is revisiting nuclear options—from floating power plants for remote grids to shipboard reactors for large-vessel propulsion [1]. Among advanced concepts, the Molten Salt Reactor (MSR) is frequently discussed for marine deployment because it can operate at high temperature and near-atmospheric pressure, enabling compact, efficient systems [2].

A defining MSR feature is liquid fuel salt, coupled with a passive shutdown concept that relies on gravity-driven draining to a geometrically subcritical drain tank [3]. However, marine platforms experience continuous six-degree-of-freedom motions (roll, pitch, yaw, heave, sway, surge) that modify the effective gravity vector and introduce non-inertial accelerations, potentially inducing free-surface sloshing, transient head losses and drain-line hold-up [4]. Incomplete draining can trap salt in the core or piping, concentrating decay heat and, in worst geometries, challenging subcriticality

This study numerically investigates the effect of representative roll conditions on MSR emergency drain dynamics using a dual-tank geometry. In the present study, an air–water surrogate system is employed by matching the geometry and operating conditions of an experimental apparatus currently under construction.

2. Methods and Results

2.1 Geometry and solver setup

Fig.1 shows the computational domain of dual-tank emergency drain system, with key dimensions summarized. The coordinate origin is defined at the bottom center of the LFS tank. The LFS tank is assumed to be located near the ship's center of gravity.

The initial liquid level in the LFS tank is 0.384 m, and all drain lines have a 3° downward inclination. Each branch line contains two freeze valves and multiple elbows (1×93°, 7×90°, 3×87°). Freeze valves are assumed fully open, while their geometric losses are included. An equalizer line provides a cover-gas path for pressure equalization; to avoid asymmetric pressure conditions, each drain tank is connected separately to the upper region of the system.

Transient simulations are performed in ANSYS Fluent 2025 R2 using a pressure-based solver and VOF for the air–liquid interface. Water and air are used as surrogate fluids at room temperature and atmospheric pressure, with turbulence modeled by k–ω SST and implicit time integration. The mesh comprises 1.41M polyhedral cells with four inflation layers. The time step is 0.025 s, reduced to 0.01 s after 140 s.

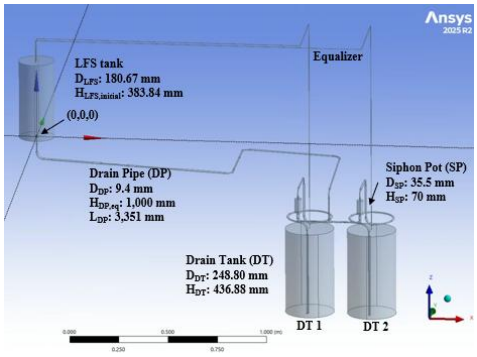

Fig. 1. Computational domain of dual-tank drain system.

2.2 Rolling kinematics & Additional Force Model

The platform roll was prescribed as a single-degree-of-freedom harmonic rotation about the x-axis with a fixed period T = 5 s. Roll amplitudes of 20° and 30° were simulated at the same period to isolate the effect of roll intensity. The governing equations were solved in a fixed computational frame, while the effects of roll motion were incorporated using a user-defined function (UDF) by (i) applying a time-varying gravity vector consistent with the instantaneous roll angle and (ii) adding rotational body-force source terms (centrifugal, tangential/Euler, and Coriolis) to the momentum equations.

3. Results

Fig. 2 depicts the liquid velocity measured at a drain-line monitoring location immediately below the LFS tank outlet for three cases: no rolling, 20° rolling, and 30° rolling, with a fixed roll period of T = 5 s. In the rolling cases, the velocity signal shows distinct periodic oscillations synchronized with the imposed platform motion, indicating that the local discharge flow is directly modulated by the time-varying effective gravity vector and the resulting changes in driving head at the tank exit. As the roll amplitude increases from 20° to 30°, the fluctuation amplitude becomes more pronounced, demonstrating stronger unsteady forcing of the draining

process. Near drain termination, the onset and intensification of gas–liquid two-phase flow lead to increased unsteadiness and amplified velocity fluctuations.

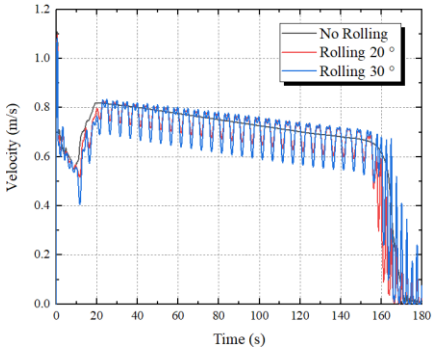

Fig. 2. Comparison of Drain Velocity at Drain pipe.

Late in the draining process, the outlet can lose submergence, leading to repeated exposure and triggering gas–liquid two-phase flow in the drain pipe. This breaks the continuous liquid column and disrupts sustained discharge; consequently, larger motion amplitudes leave more liquid in the LFS tank (at 180 s: No motion < Roll 20° < Roll 30°) as shown in Fig.3.

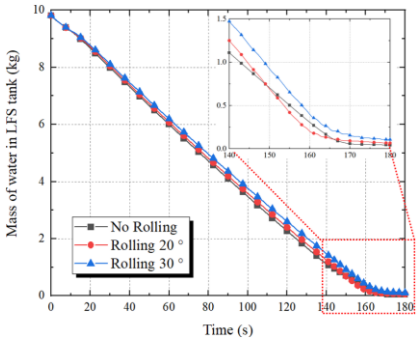

Fig. 3. Mass of Water in LFS tank.

Using separate equalizer lines can make one branch longer, increasing gas-line losses and delaying venting. The resulting higher pressure can provides back-pressure that suppresses liquid inflow. At 180 s, mass of water in DT-1 exceeds DT-2 by +2.13% (No motion), +1.47% (Roll 20°), and +2.76% (Roll 30°).

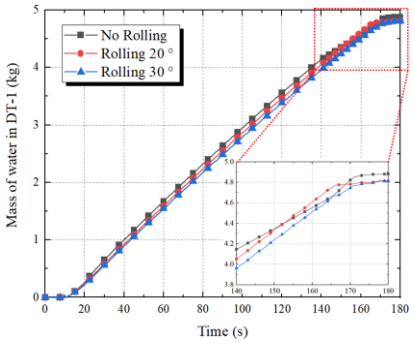

Fig. 4. Mass of Water in Drain Tank 1.

At 20°, the motion-induced unsteadiness partially attenuates the inventory imbalance, whereas at 30° it can amplify the imbalance.

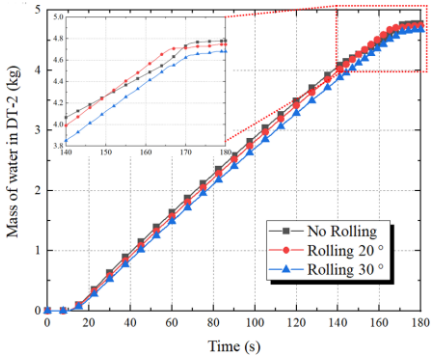

Fig. 5. Mass of Water in Drain Tank 2.

4. Conclusions and Future Works

This study used VOF-based CFD to evaluate a dual-tank MSR emergency drain system under roll motion. Rolling motion periodically alters the effective gravity direction and driving head, amplifying discharge unsteadiness and promoting late-stage two-phase intermittency, which delays draining and increases residual hold-up. Separate equalizer lines can add unequal gas-line losses, creating back-pressure that biases tank inventories and causes DT-1/DT-2 imbalance. Validation will be performed by comparing the CFD predictions with drainage results from the experimental apparatus under the **no-rolling** condition, and the model will then be extended to simulations using **prototypic molten-salt properties**.

ACKNOWLEDGMENTS

This work was supported by Korea Institute of Energy Technology Evaluation and Planning(KETEP) grant funded by the Korea government(MOTIE)(RS-2024-00403194).

REFERENCES

[1] M. Drosińska–Komor, J. Głuch, N. Ziółkowska, K. Brzezińska–Gołębiewska, J. Blaut, and P. Ziółkowski, Integrating fourth–generation reactors into maritime transport, Ocean Eng., Vol. 342, p. 122891, 2025.
[2] L. G. de Freitas Neto, L. O. Freire, A. dos Santos, and D. A. de Andrade, Potential advantages of molten salt reactor for merchant ship propulsion, Brazilian J. Radiat. Sci., Vol. 9, no. 2B (Suppl.), 2021.
[3] D. Gérardin, M. Allibert, D. Heuer, A. Laureau, E. Merle-Lucotte, and C. Seuvre, Design evolutions of the molten salt fast reactor, International Conference on Fast Reactors and Related Fuel Cycles: Next Generation Nuclear Systems for Sustainable Development (FR17), June 26-29, 2017, Yekaterinburg, Russian Federation.
[4] S. Park, S. Kim, G. A. K. M. R. Bari, and J.H. Jeong, Fundamental understanding of marine applications of molten salt reactors: Progress, case studies, and safety, J. Mar. Sci. Eng., Vol. 12, no. 10, p. 1835, 2024.